Supplemental Information of

Molecular Dynamics Simulations on Human Beta Defensin Type 3 Crossing Different Lipid Bilayers

Rabeta Yeasmin, Ann Brewer, Lela R Fine, Liqun Zhang*

Chemical Engineering department, Tennessee Technological University, Cookeville, TN, 38505

1. Tables:

Table S1. All-atom system set up and simulation details.

hBD-3 wildtype	Lipid leaflet (Top + Bottom)	Lipid number	Water number	Simulation time (ns)	Size of simulation box ($Å^3$)
Tetramer	0	0	20821	400	114.9x67.4x86.8
Tetramer	POPC+POPC	100+100	26965	100	101.2x101.2x118.7
Tetramer	POPS+POPS	100+100	23591	100	95.2x95.2x120.9
Bilayer	POPS+POPS	72+72	4845	20	65.9x65.9x73.4
Bilayer	POPC+POPC	100+100	9042	20	82.6x82.6x76.7

Table S2. US system setup and simulation details.

hBD-3 analogue	Lipid leaflet (Top + Bottom)	Lipid number	hBD-3/Lipid number ratio	Window number	Water thickness (Å)	Simulation time (ns)
Monomer	POPC+POPC	100+100	1:200	49	60	1000
	POPS+POPS	100+100	1:200	49	60	1000
	POPS+POPC	114+100	1:214	49	60	1000
Dimer	POPC+POPC	100+100	1:100	61	68	1000
	POPS+POPS	100+100	1:100	61	68	1000
	POPS+POPS (GROMACS)	**100+100**	**1:100**	**61**	**110**	**1000**
	POPS+POPC	114+100	1:107	61	68	1000
Tetramer	POPC+POPC	300+300	1:150	69	78	1000
	POPS+POPS	300+300	1:150	69	78	1000
	POPS+POPC	341+300	1:160	69	78	2000

Table S3. NAMD run US system box size information.

hBD-3 analogue	Lipid leaflet (Top + Bottom)	Box Size (Å3)
Monomer	POPC+POPC	87.1x81.1x168.2
	POPS+POPS	75.7x90.8x173.7
	POPS+POPC	86.0x86.0x157.6
Dimer	POPC+POPC	90.5x79.6x181.8
	POPS+POPS	84.6x84.6x170.0
	POPS+POPC	88.4x85.8x168.2
Tetramer	POPC+POPC	143.4x143.4x244.1
	POPS+POPS	145.4x143.8x236.2
	POPS+POPC	147.9x147.9x241.4

2. Figures:

hBD-3 (PDB ID: 1KJ6): GIINTLQKYYC$^{(1)}$RVRGGRC$^{(2)}$AVLSC$^{(3)}$LPKEEQIGKC$^{(4)}$STRGRKC$^{(5)}$C$^{(6)}$RRKK; (+11)
Disulfide bonding: C$^{(1)}$-C$^{(5)}$, C$^{(2)}$-C$^{(4)}$, C$^{(3)}$-C$^{(6)}$

Figure S1. hBD-3 sequence, charge and disulphide bonding pattern.

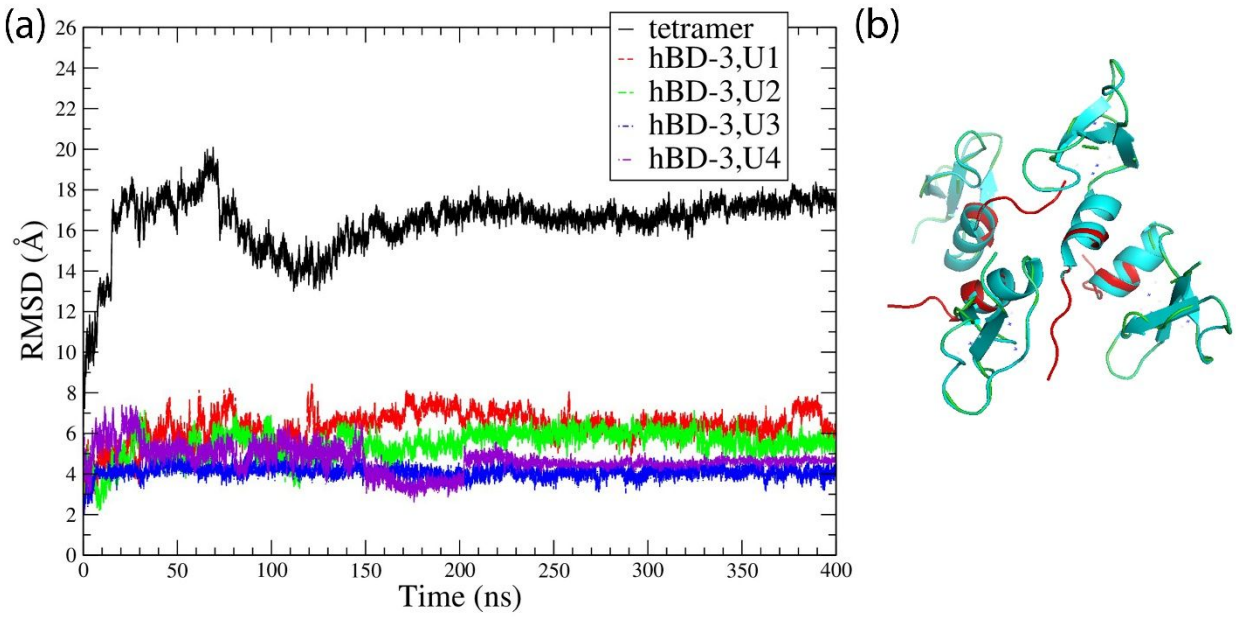

Figure S2. RMSD comparison of hBD-3 tetramer and its individual unit (**a**), after aligning the trajectories on the initially orderly packed structure in 400 ns. hBD-3, U1 is the abbreviation of the first hBD-3 unit in the tetramer; hBD-3, U2 is the second hBD-3 unit in the tetramer, and so on, and (**b**) comparison of the tetramer structure at 200 ns (cyan and red) and 400 ns (green).

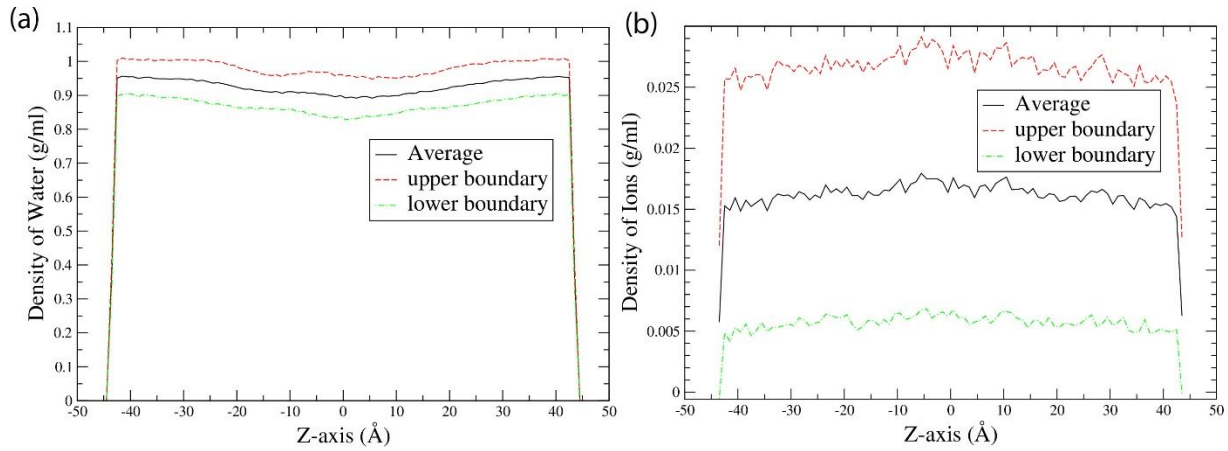

Figure S3. Water mass density (**a**) and ion mass density (**b**) along z-axis in the tetramer all-atom simulation.

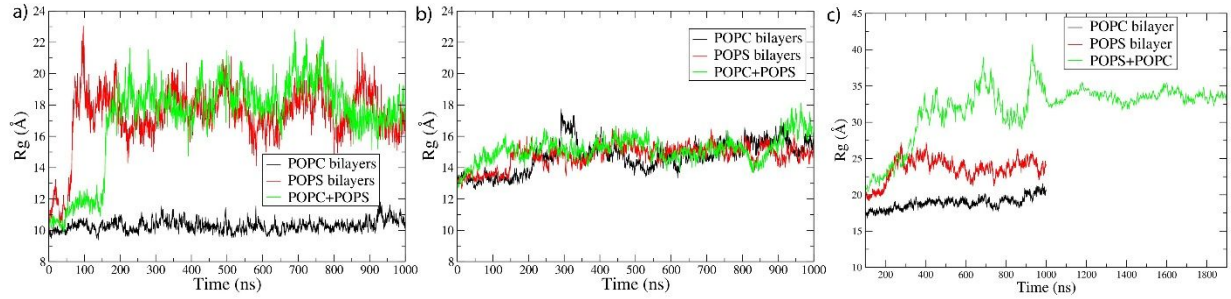

Figure S4. R_g of hBD-3 monomer (**a**), dimer (**b**) and tetramer (**c**) in three kinds of lipid bilayers at 0 Å window.

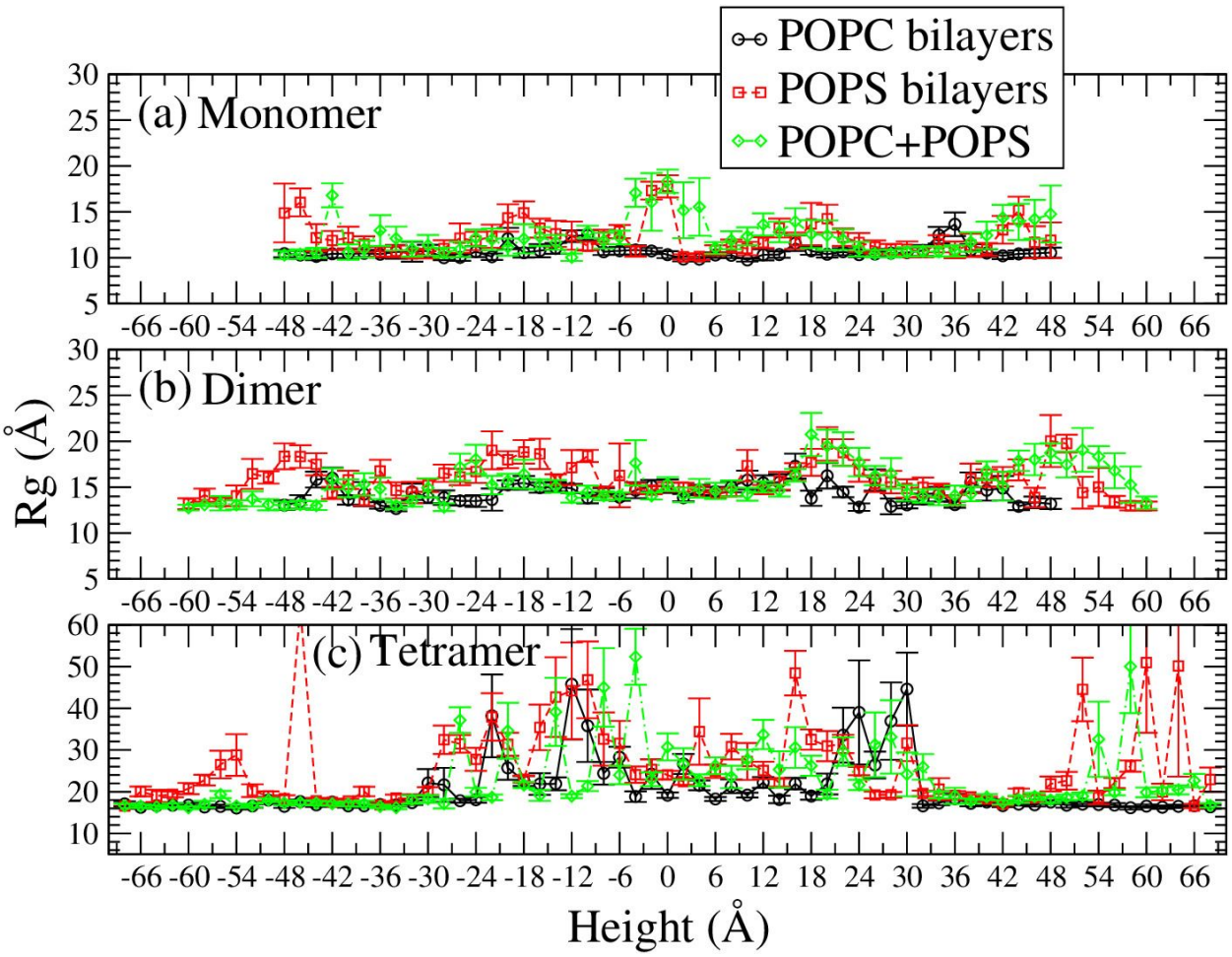

Figure S5. Averaged R_g of hBD-3 monomer (**a**), hBD-3 dimer (**b**) and hBD-3 tetramer (**c**) over the last 700 ns simulations at different windows.

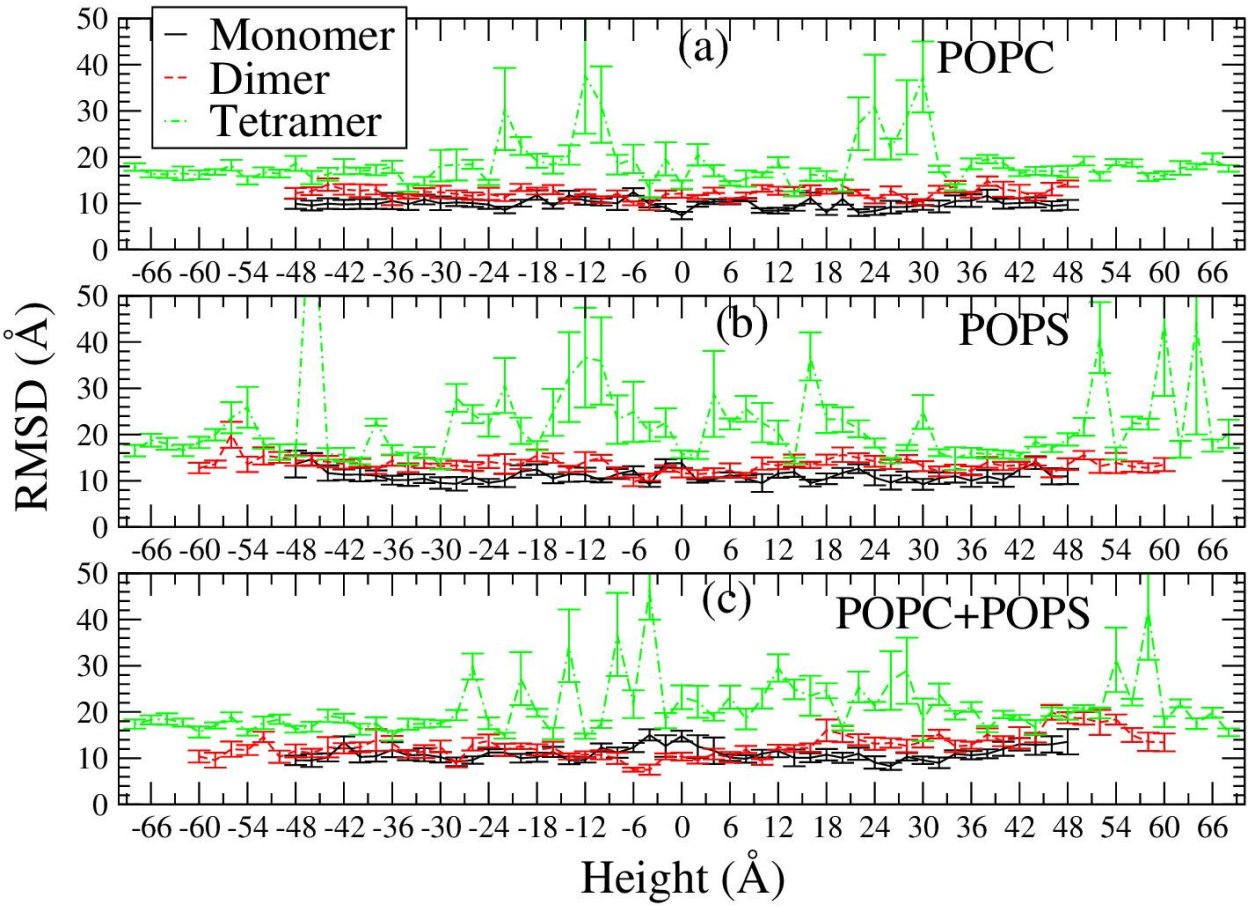

Figure S6. Average RMSD and standard deviation result for hBD-3 monomer, dimer and tetramer in POPC bilayer (**a**), POPS bilayer (**b**), and POPC+POPS lipid bilayer (**c**) in different windows based on last 700 ns trajectory each.

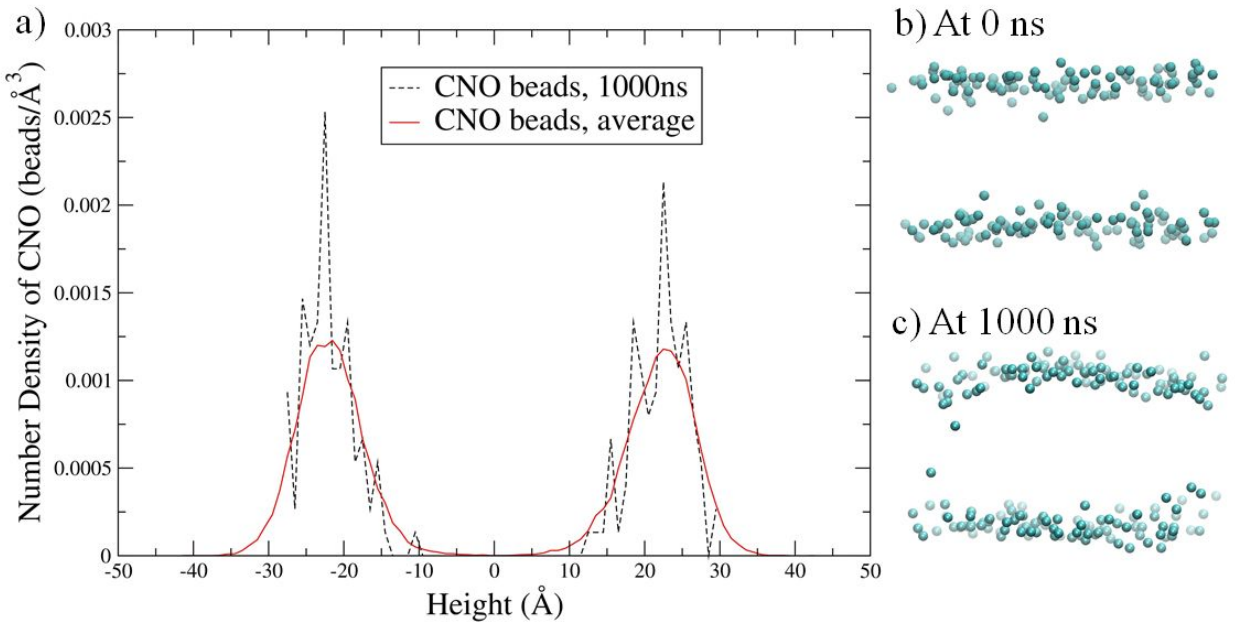

Figure S7. The average number density and the number density of CNO beads at 1000 ns (**a**), the distribution of CNO beads in the hBD-3 dimer in POPS lipid bilayer at (**b**) 0 ns and (**c**) 1000 ns at 0 Å window.

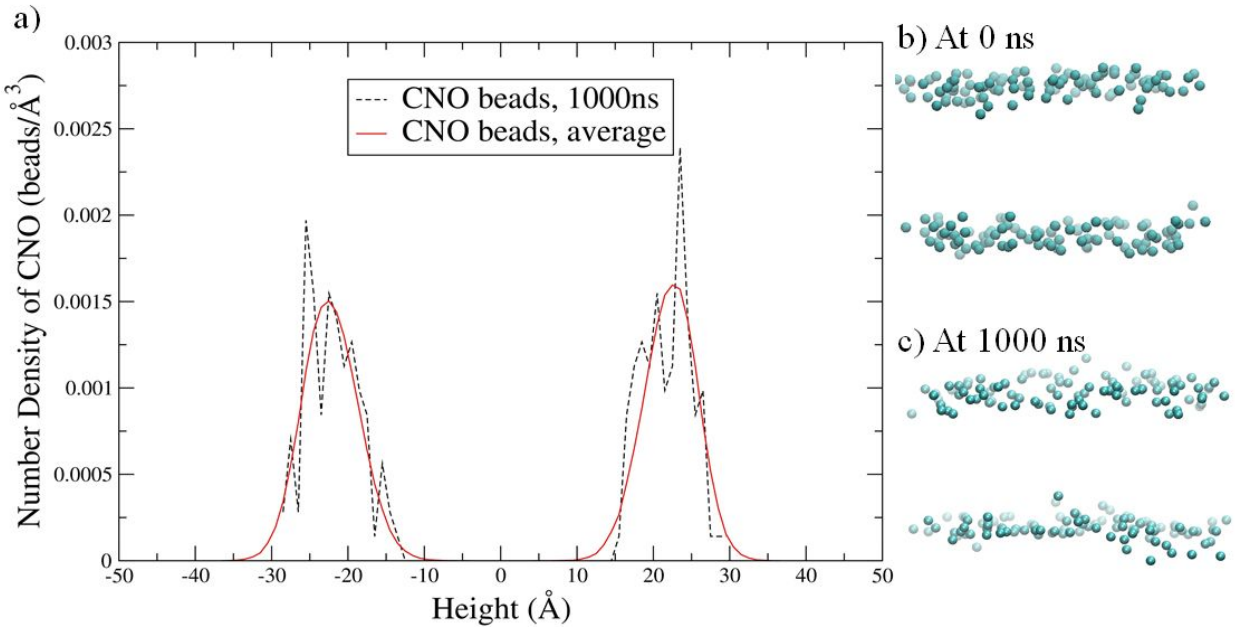

Figure S8. The average number density and the number density at 1000 ns (**a**); the distribution of CNO beads in hBD-3 monomer in POPS lipid bilayers system at (**b**) 0 ns and (**c**) 1000 ns at 0 Å window.

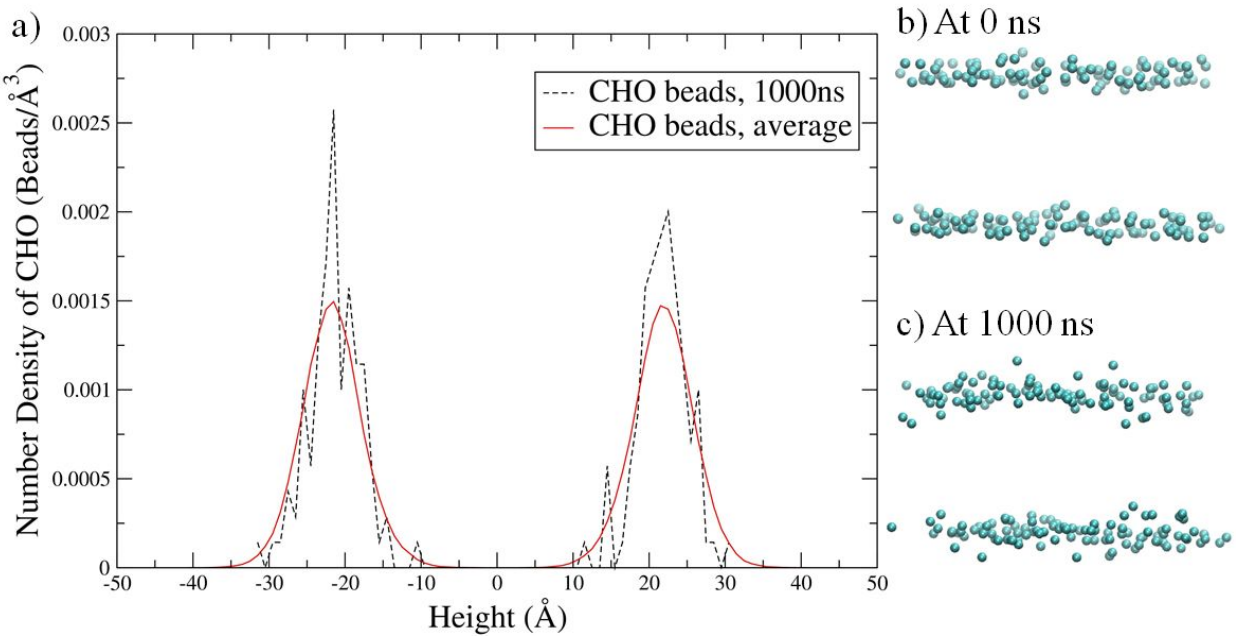

Figure S9. The number density of CHO beads at (**a**) 1000 ns and CHO beads distribution in the hBD-3 monomer in POPC bilayer system at (**b**) 0 ns and (**c**) 1000 ns at 0 Å window.

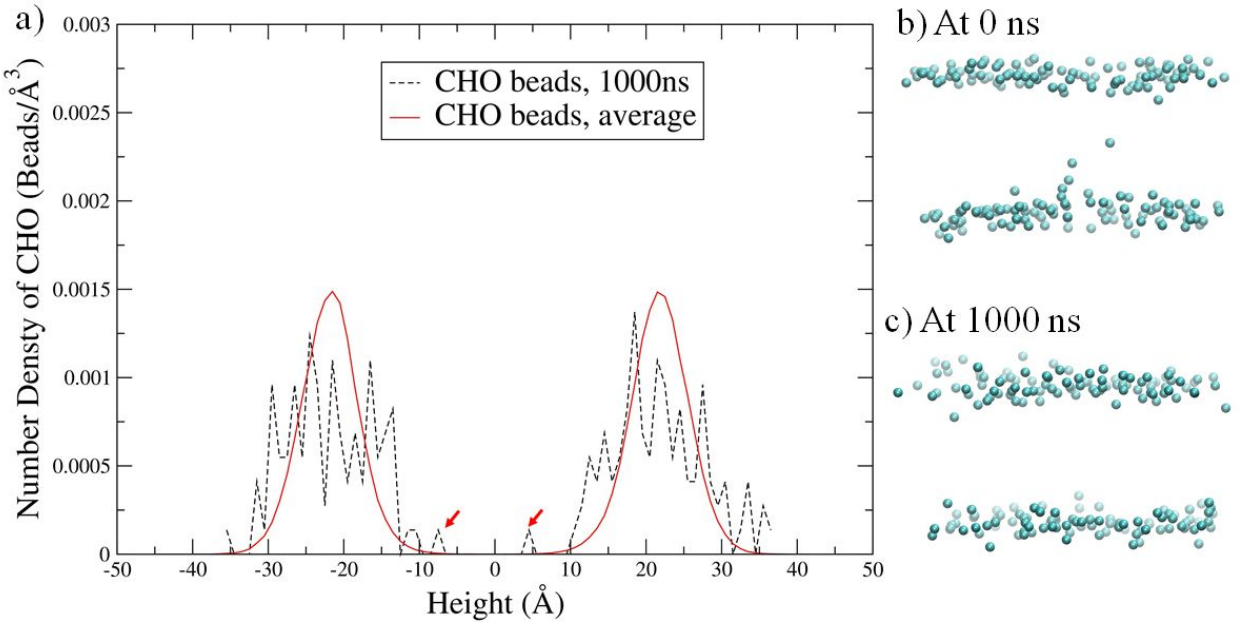

Figure S10. The number density of CHO beads at (**a**) 1000 ns and CHO beads distribution in the hBD-3 dimer in POPC bilayer at (**b**) 0 ns and (**c**) 1000 ns at 0 Å window.

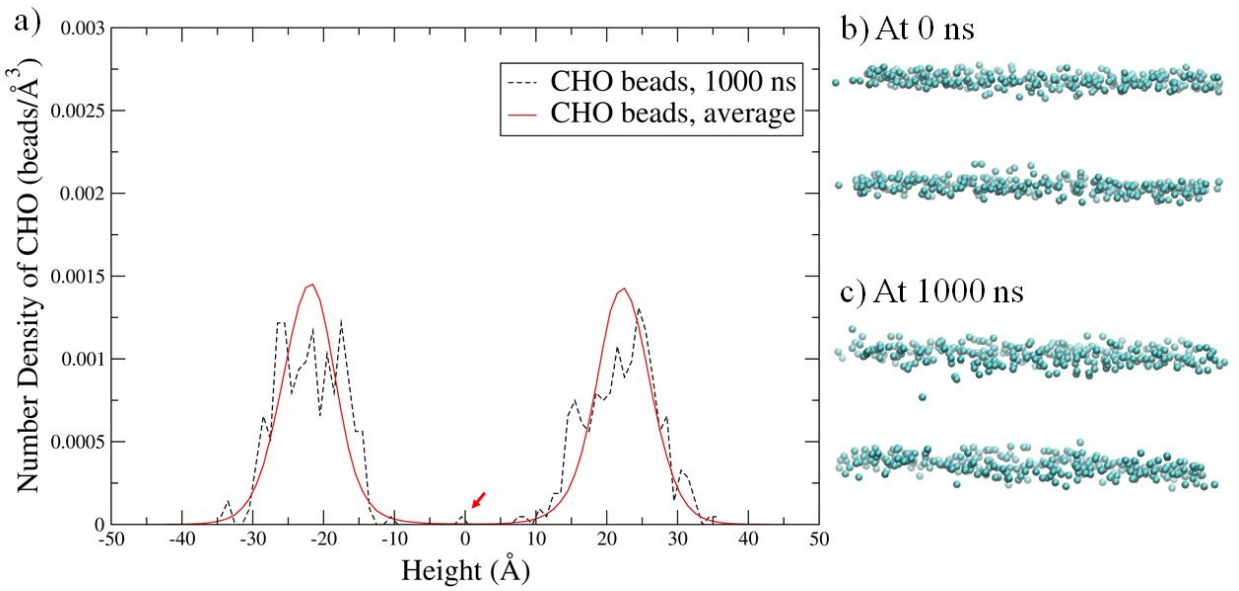

Figure S11. The average number density of CHO beads on POPC lipids in hBD-3 tetramer system during 1000 ns simulations (**a**), and CHO beads distribution in the hBD-3 tetramer in POPC bilayer system at (**b**) 0 ns and (**c**) 1000 ns at 0 Å window.

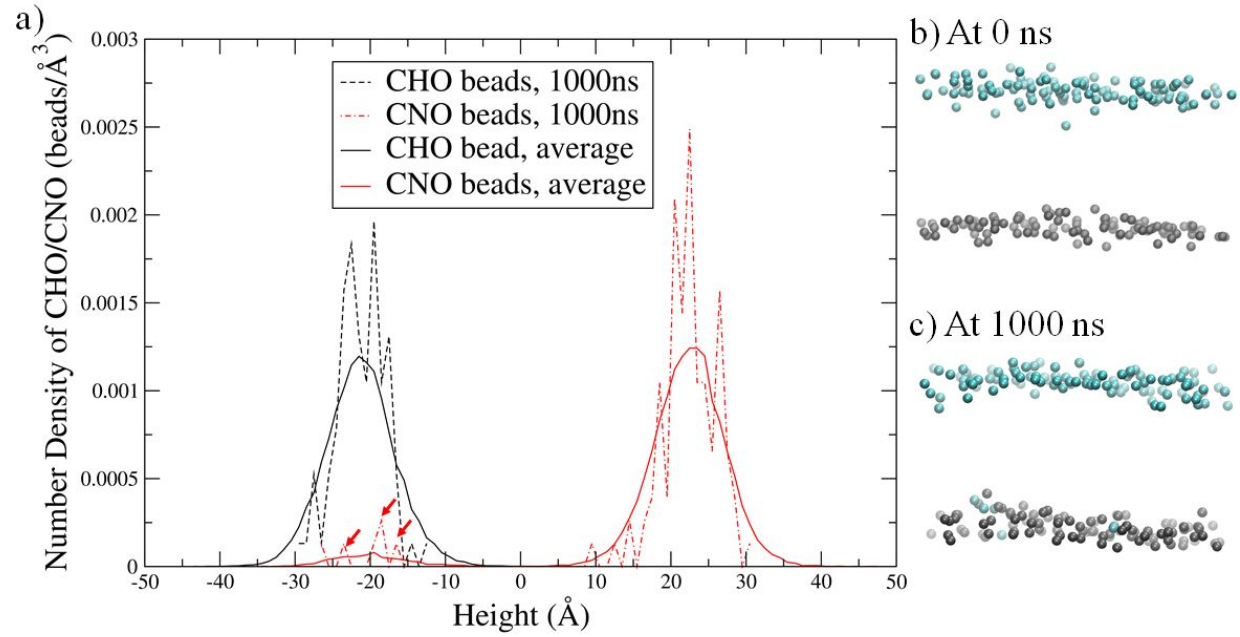

Figure S12. The number density profile of CNO and CHO beads on POPS + POPC lipid bilayer in the hBD-3 monomer system at the 0 Å window at 1000 ns, with the number density of CNO beads diffused to the POPC leaflet pointed out using red arrows(**a**), and the distribution of CNO (in blue) and CHO (in chocolate) beads in the monomer system (all other molecules not shown) at (**b**) 0 ns and at (**c**) 1000 ns. In (c), the CNO beads moved to the CHO beads side were clear.

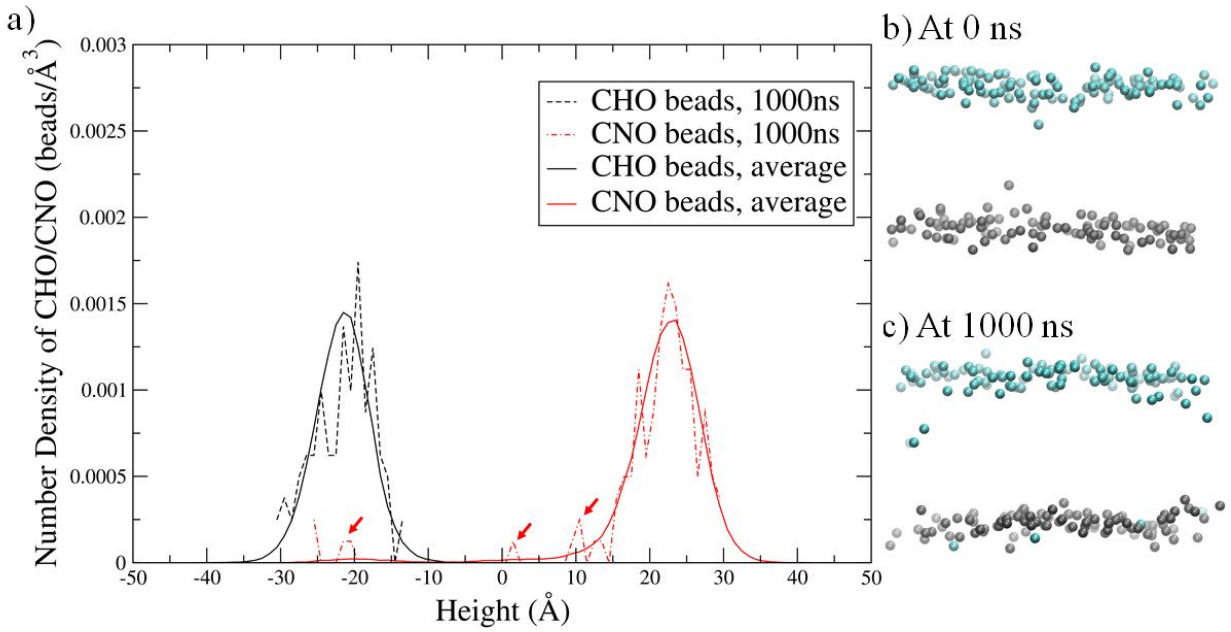

Figure S13. The number density profile of CNO and CHO beads on POPS+POPC lipid bilayer in the hBD-3 dimer system at 0 Å window at 1000 ns, with the number density of CNO beads diffused to the POPC leaflet pointed out using red arrows (**a**), and the distribution of CNO (in blue) and CHO (in chocaloate) beads in the dimer system (all other molecules not shown) at 0 ns (**b**) and at 1000 ns (**c**). In c), the CNO beads moved to th CHO beads side was clear.

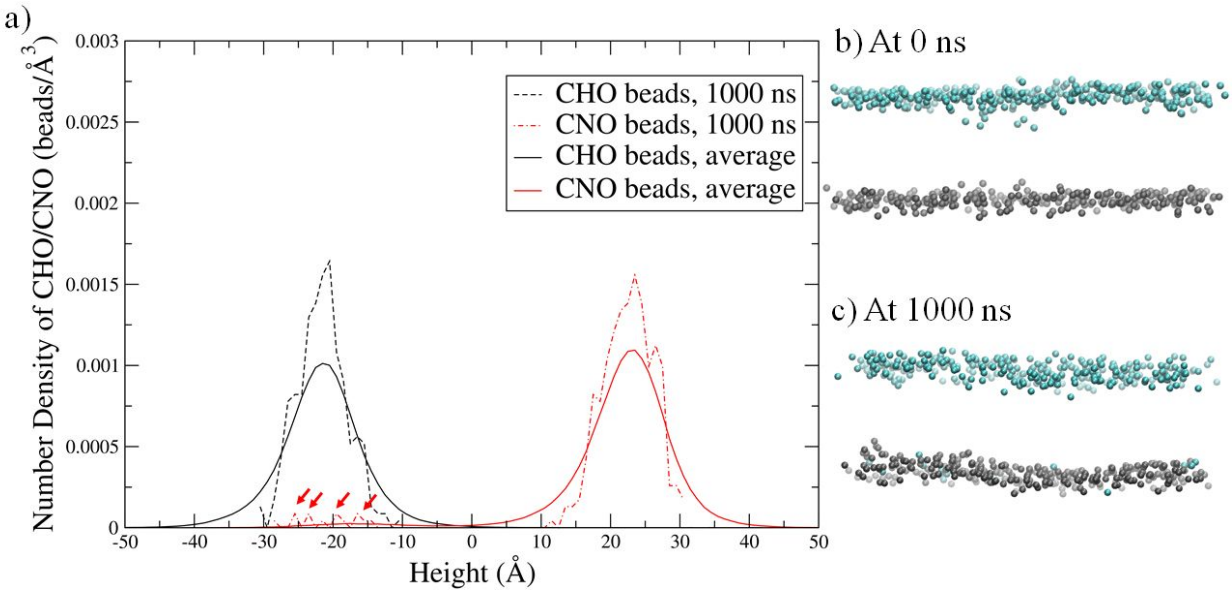

Figure S14. The number density profile of CNO and CHO beads on the POPS+POPC lipid bilayer in the hBD-3 tetramer system at the 0 Å window at 1000 ns, with the number density of CNO beads diffused to the POPC leaflet pointed out using red arrows(**a**), and the distribution of CNO (in blue) and CHO (in chocolate) beads in the tetramer system (all other molecules not shown) at (**b**) 0 ns and at (**c**) 1000 ns . At 1000 ns, the CNO beads moved to the CHO beads side were clear.

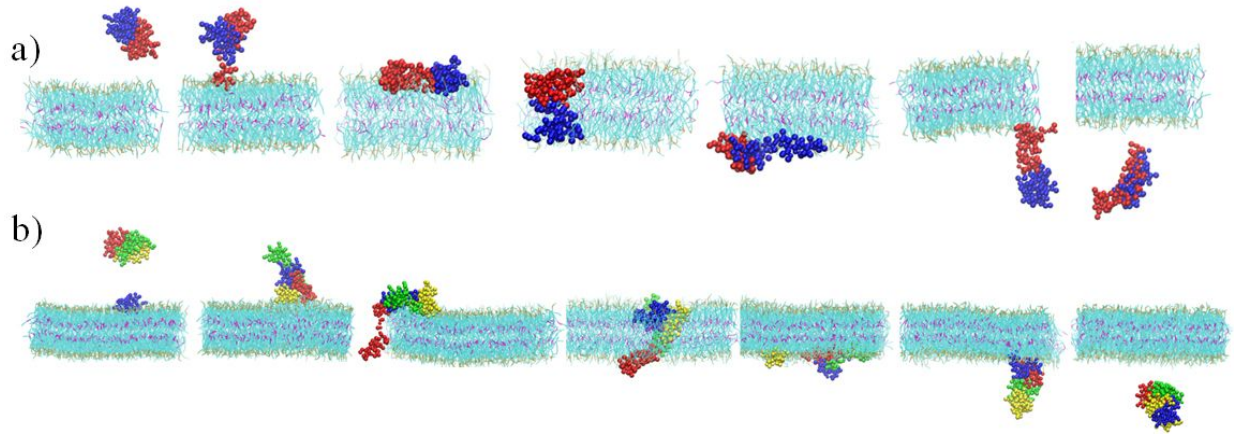

Figure S15. hBD-3 oligomer structure around POPS lipid bilayer after 1000 ns simulations. (**a**) hBD-3 dimer on POPS lipid bilayer at the heights of 60 Å, 48 Å, 24 Å, 0 Å, -24 Å, -48 Å, and -60 Å from left to right; (**b**) hBD-3 tetramer at heights of 68 Å, 48 Å, 24 Å, 0 Å, -24 Å, -48 Å, and -68 Å from left to right.

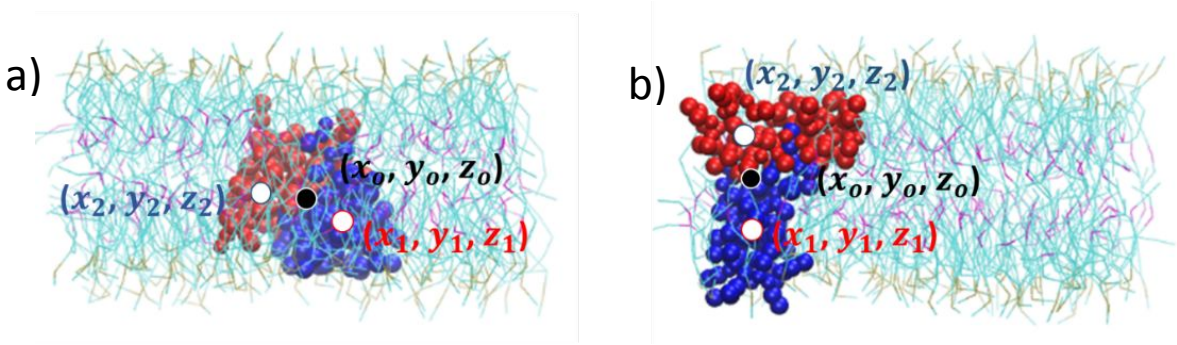

Figure S16. hBD-3 dimer at 0 Å window has the COM of each individual unit as $\{(x_{1.}\ y_1{,}z_1$) and $(x_{2.}\ y_2{,}z_2)\}$ and the whole oligomer COM as $(x_{o.}\ y_o{,}z_o)$ in two cases (**a**) and (**b**). RMSZ will be lower for the orientation of the dimer units in (**a**) than in (**b**).

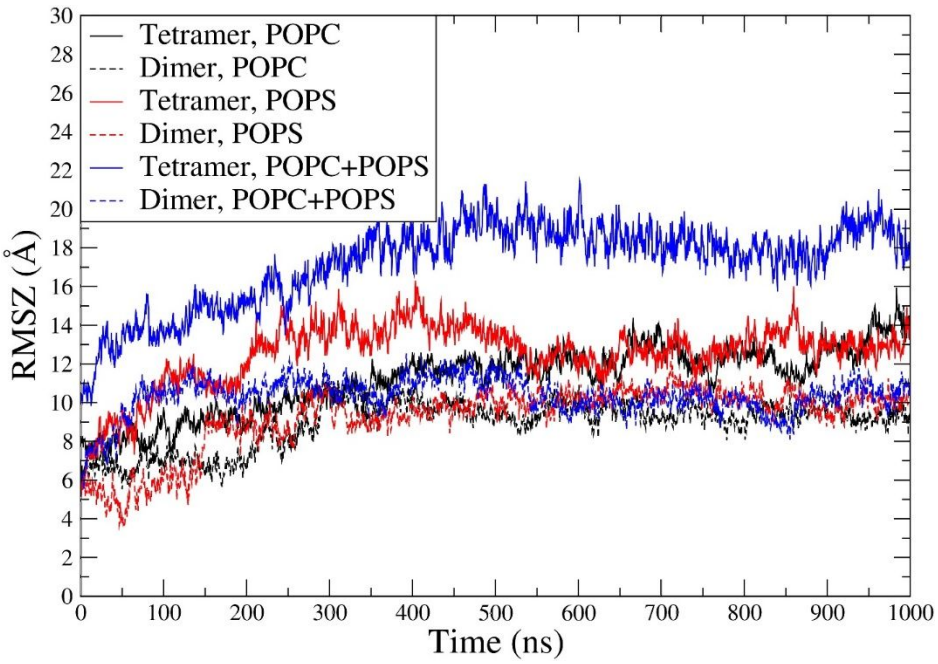

Figure S17. RMSZ of hBD-3 tetramer (in solid line) and dimer (in dashed line) in POPC bilayer (in black), in POPS bilayer (in red) and in POPS+POPC mixed bilayer (in blue) at 0 Å windows during 1000 ns simulations.

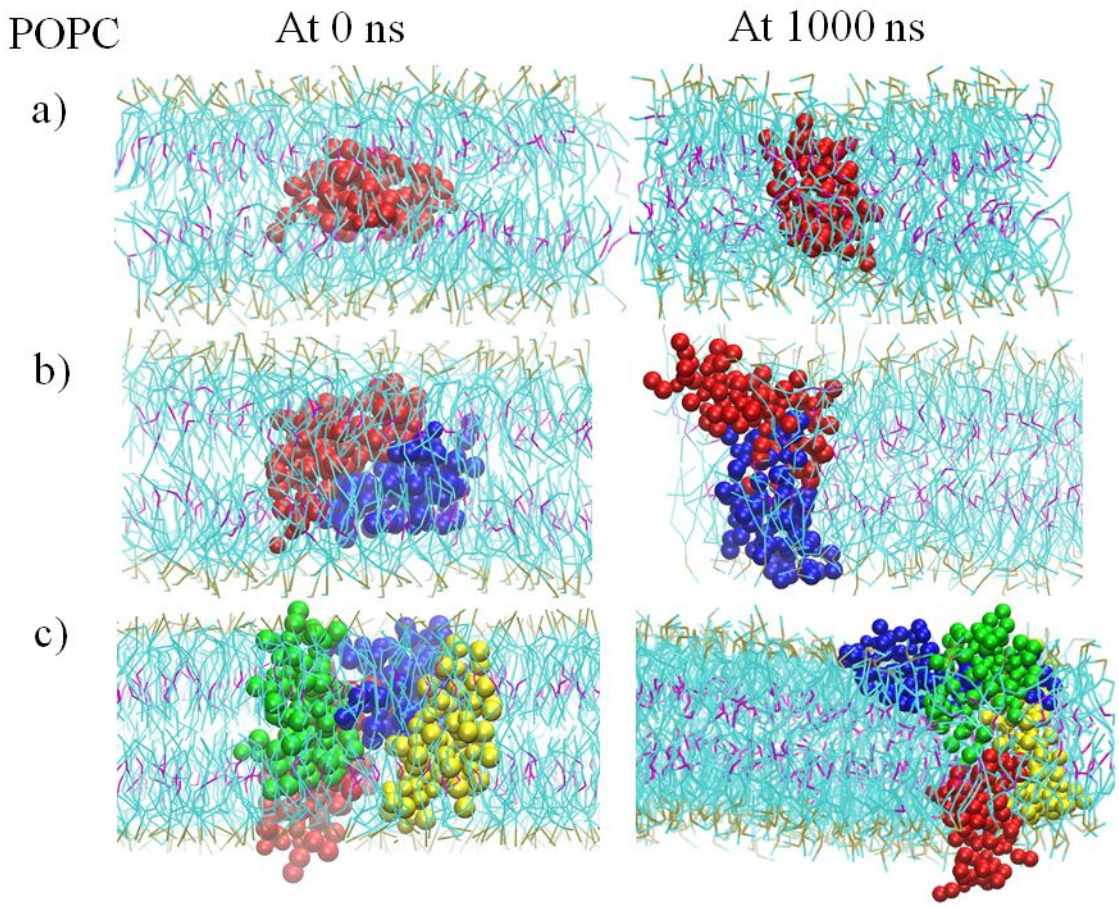

Figure S18. hBD-3 monomer (**a**), dimer (**b**), and tetramer (**c**) in POPC lipid bilayer at the 0 Å window at 0 ns (left column) and 1000 ns (right column).

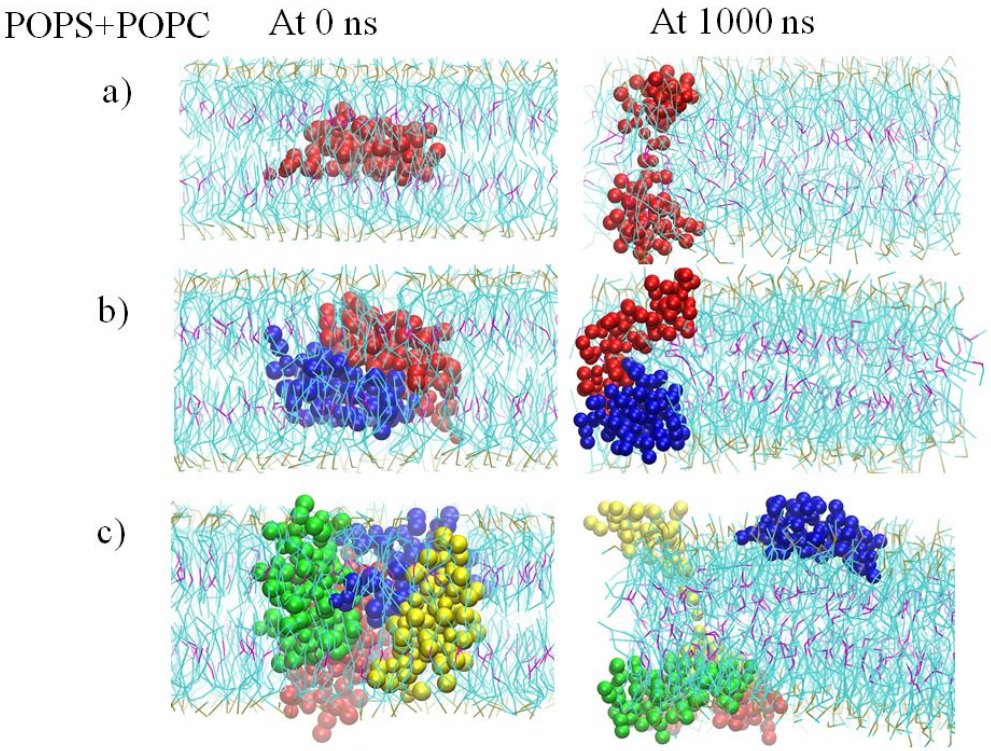

Figure S19. hBD-3 monomer(**a**), dimer(**b**), and tetramer(**c**) in POPS (top leaflet) + POPC (bottom leaflet) lipid bilayer at the 0 Å window at 0 ns (left column) and 1000 ns (right column).

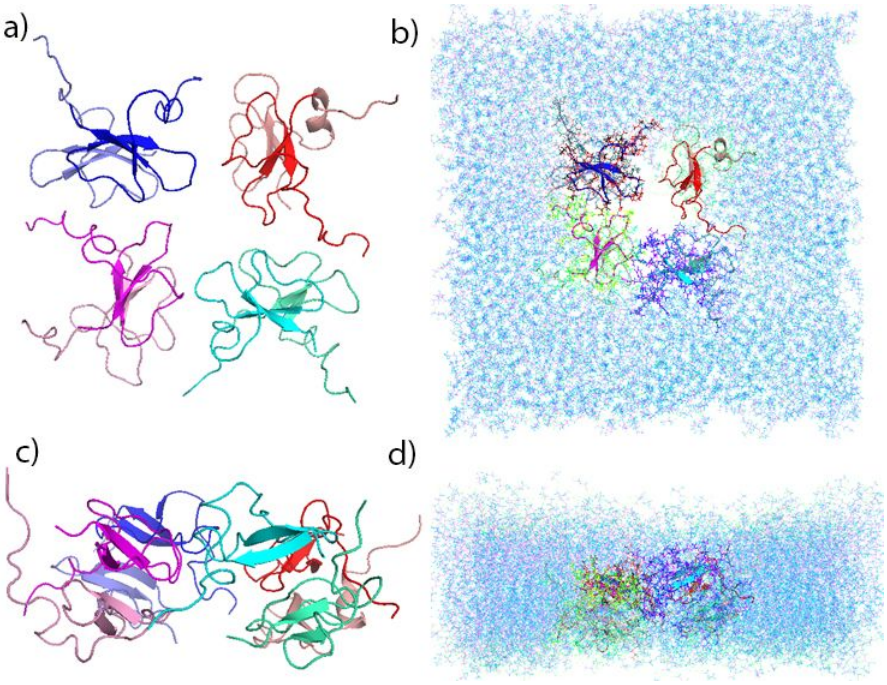

Figure S20. The octamer structure predicted using SymmDock in **a**) top view; **b**) top view inside lipid bilayer; **c**) side view; **d**) side view inside lipid bilayer.

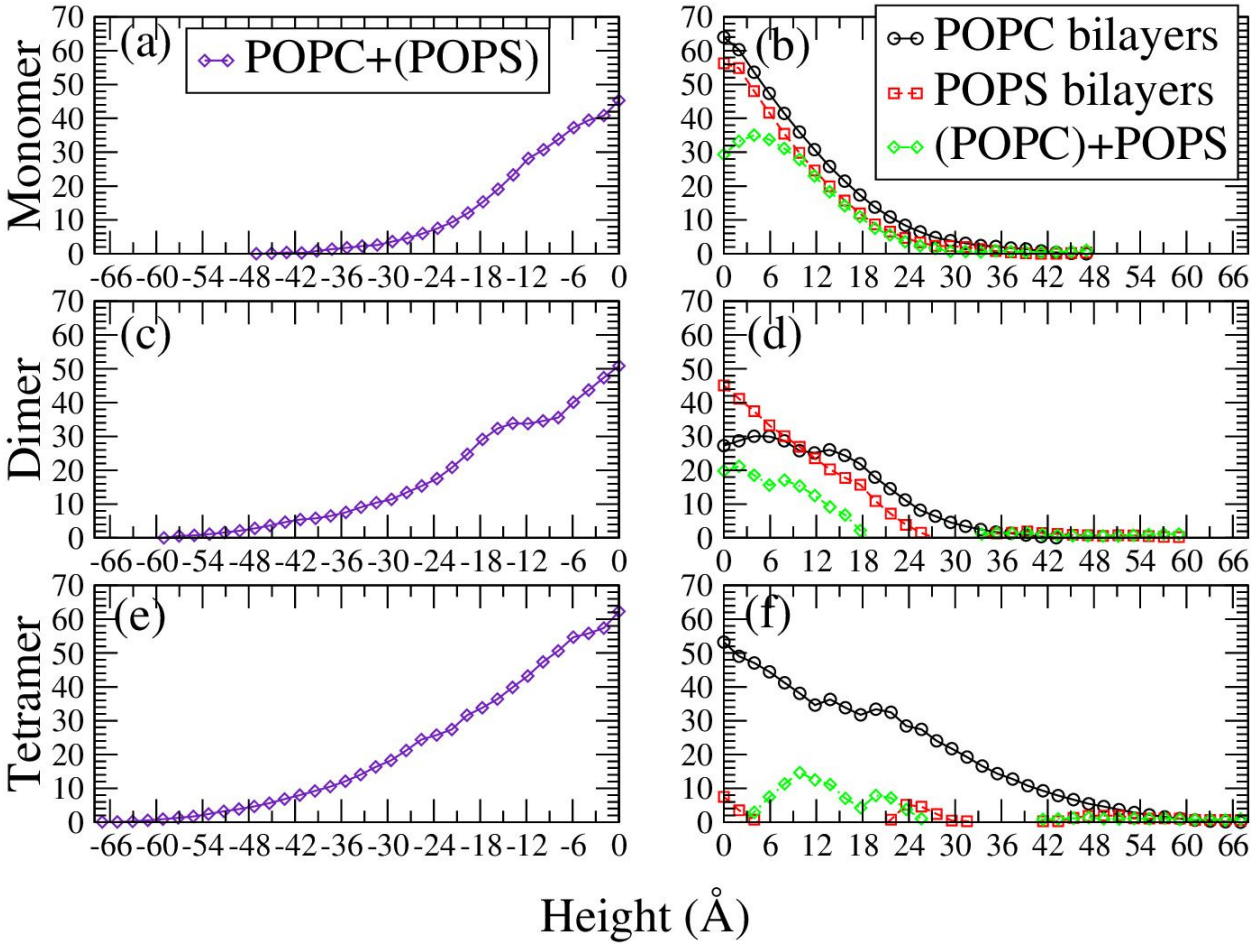

Figure S21. Translocation free energy of hBD-3 monomer crossing the POPC+POPS bilayer from the POPC leaflet (**a**) and crossing the pure POPC bilayer/POPS bilayer/POPC+POPS bilayer from the POPS leaflet (**b**), hBD-3 dimer crossing the POPC+POPS bilayer from the POPC leaflet(**c**) and crossing the pure POPC bilayer/POPS bilayers/POPC+POPS bilayer from the POPS leaflet (**d**), and hBD-3 tetramer crossing the POPC+POPS bilayer from the POPC leaflet (**e**) and crossing the pure POPC bilayer/POPS bilayer/POPC+POPS bilayer from the POPS leaflet (**f**).

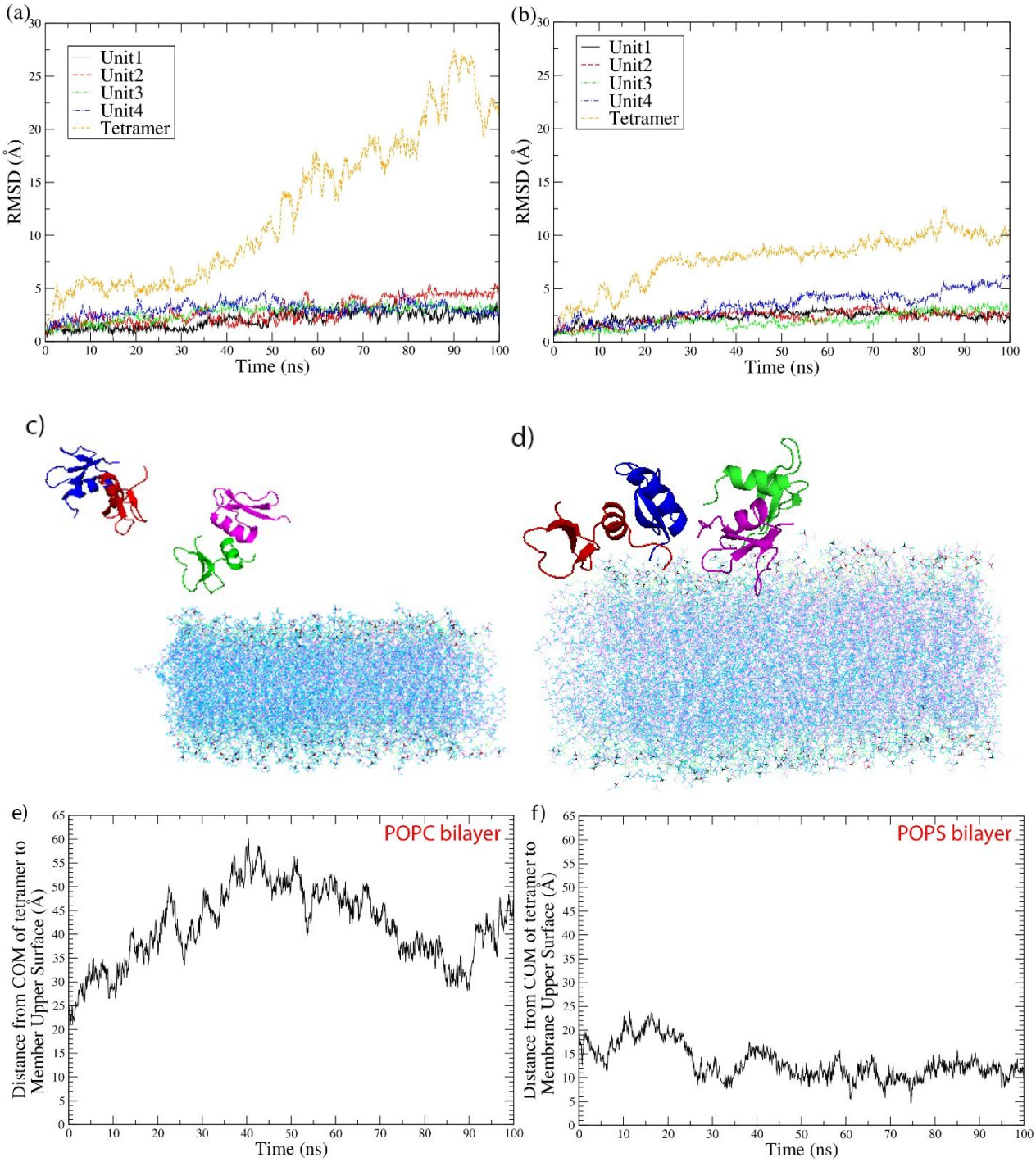
(a)
(b)
Unit1
Unit2
Unit3
Unit4
Tetramer
RMSD (Å)
Time (ns)
c)
d)
e)
f)
POPC bilayer
POPS bilayer
Distance from COM of tetramer to Member Upper Surface (Å)
Distance from COM of tetramer to Membrane Upper Surface (Å)

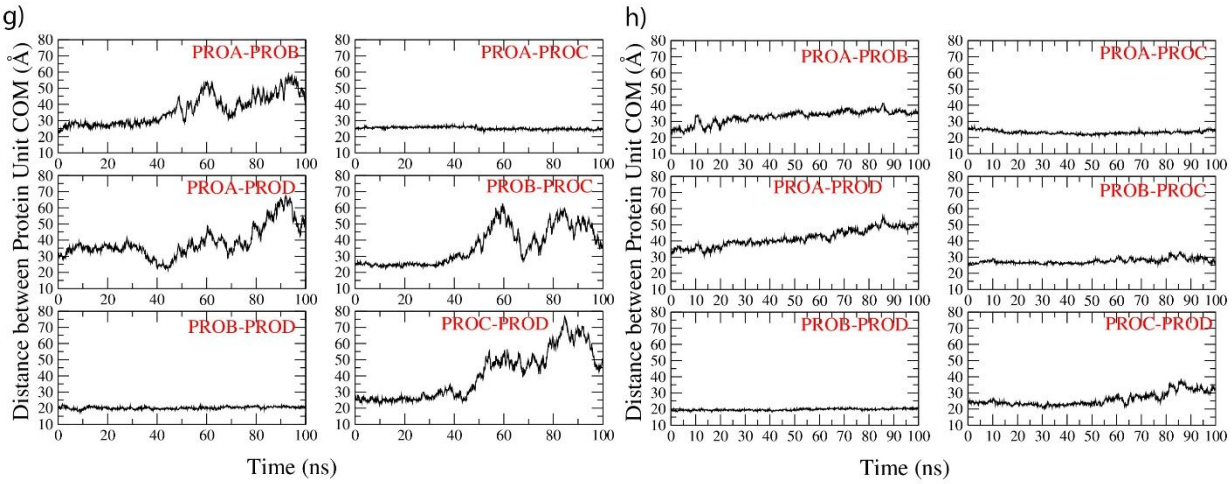

Figure S22. RMSD of the tetramer and individual units binding on POPC(**a**) and POPS (**b**) bilayer during 100 ns all-atom MD simulations, and the last structure of the tetramer binding with POPC (**c**) and POPS (**d**) lipid bilayers; the height of tetramer center of mass above the POPC (**e**) and POPS (**f**) membranes, and the distance between protein unit pairs COM in the tetramer on POPC (**g**) and POPS (**h**) membranes.

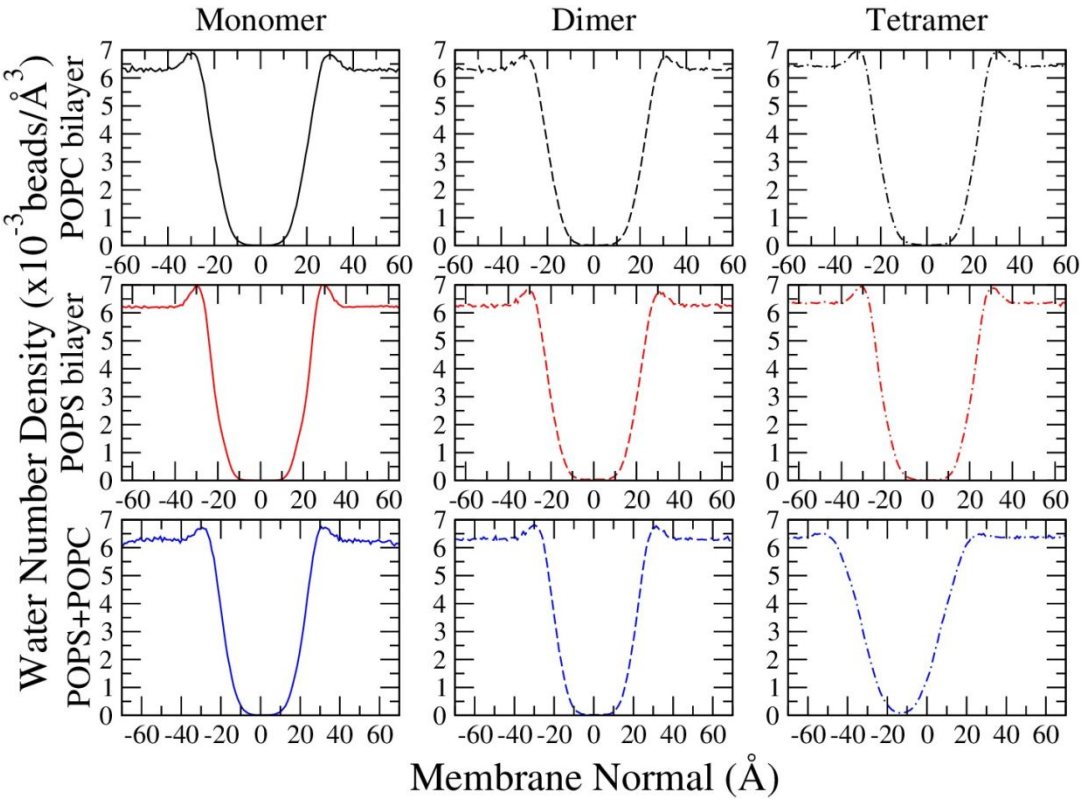

Figure S23. Water number density profiles in hBD-3 monomer/dimer/tetramer in POPC, POPS, and POPS+POPC bilayer systems at 0 Å window.

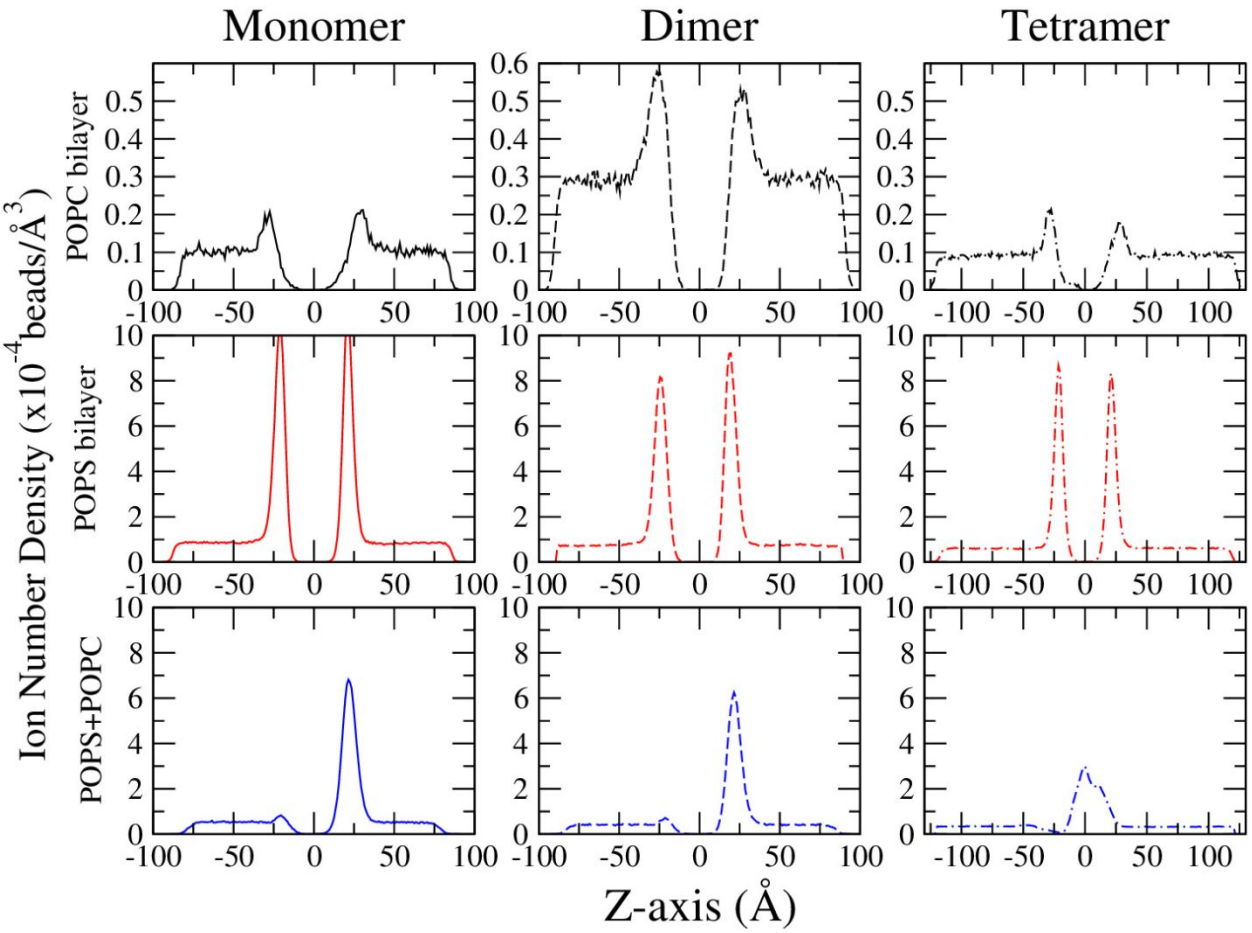

Figure S24. Ion number density profiles in hBD-3 monomer/dimer/tetramer in POPC, POPS, and POPS+POPC bilayer systems at 0 Å window.

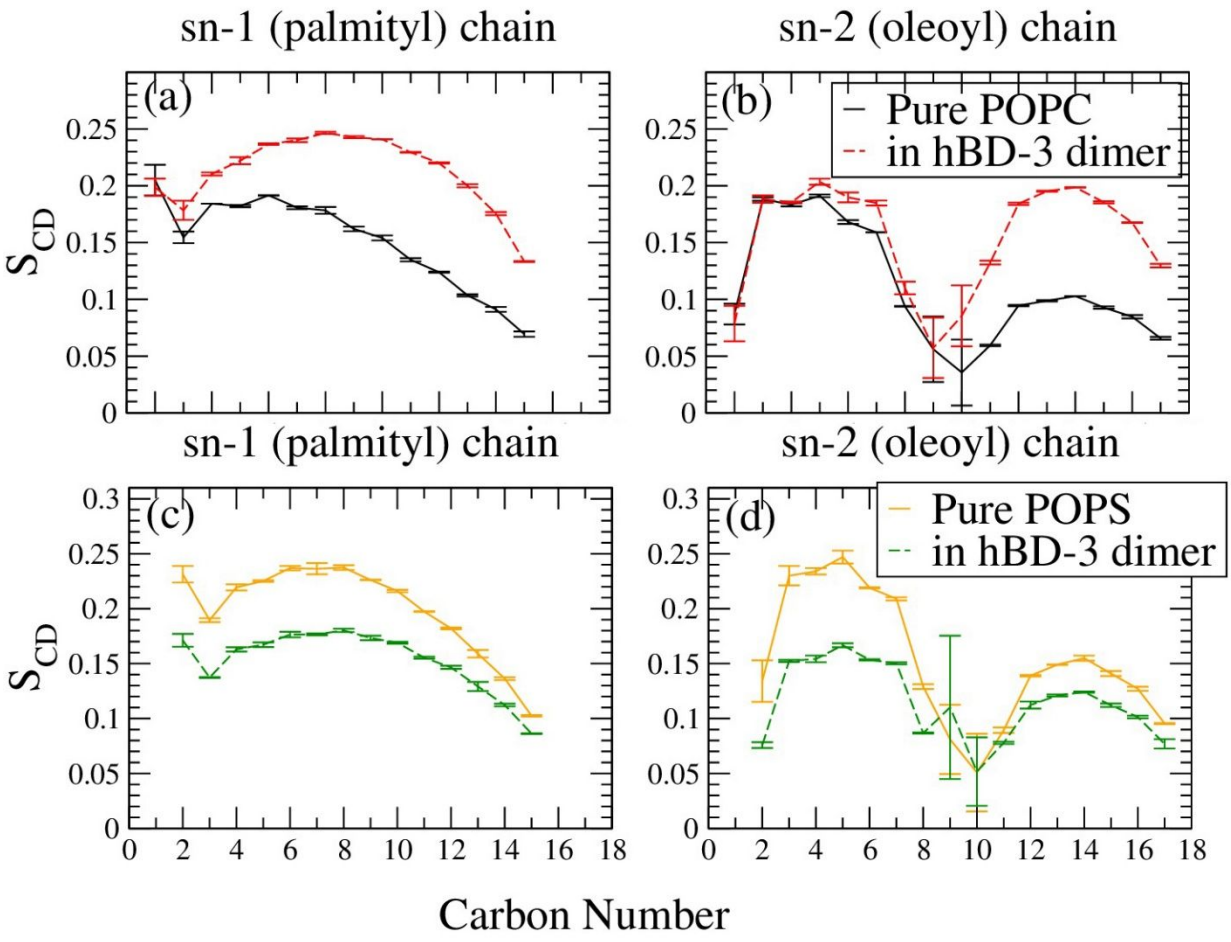

Figure S25. Comparison of order parameters of POPC lipids sn-1 chain (**a**) and sn-2 chain (**b**), and POPS lipids sn-1 chain (**c**) and sn-2 chain (**d**) in pure lipid systems and in hBD-3 dimer crossing POPC/POPS lipid bilayer US simulation systems at 0 Å window.

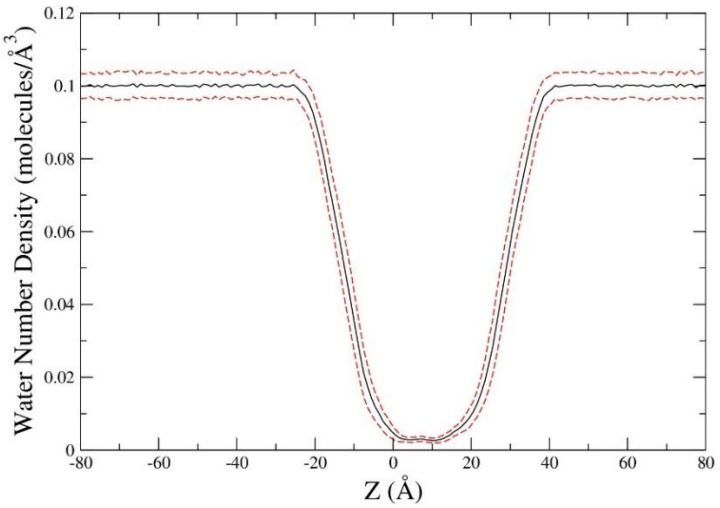

Figure S26. Water number density profile in hBD-3 dimer in wildtype in POPC lipid bilayer system at 0 Å window. The upper and lower boundaries for the average mass density are also shown in red dotted lines, in black for the average density profile.

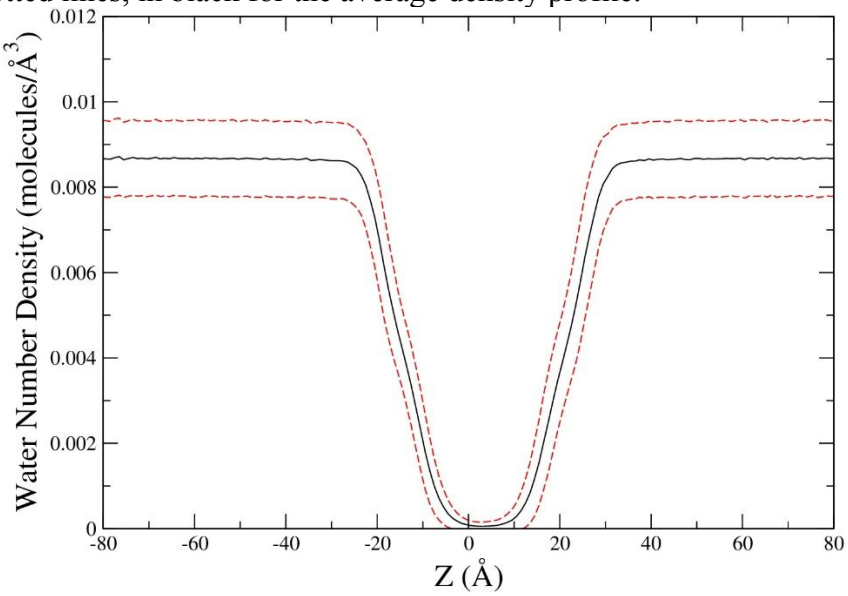

Figure S27. Water number density profile in hBD-3 dimer in wildtype in POPS lipid bilayer system at 0 Å window from Gromacs simulation. The upper and lower boundaries for the average mass density are also shown in red dotted lines, in black for the average density profile.

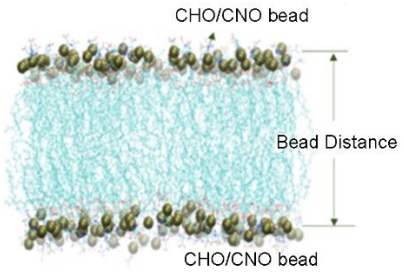

Figure S28. Membrane thickness calculation sketch. The bead distance represents the membrane thickness.

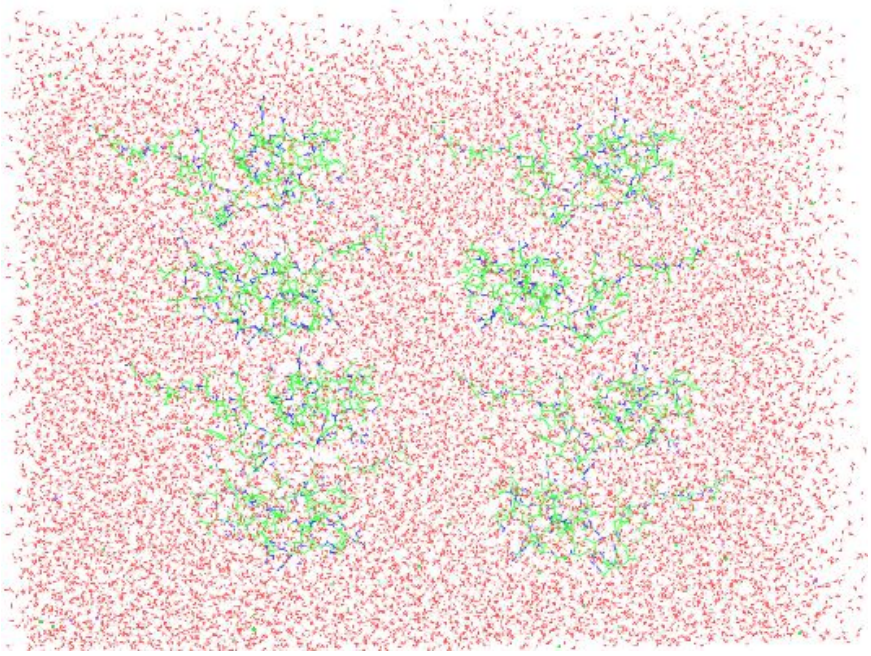

Figure S29. The snapshot of the initial simulation system on 8 hBD-3 in wildtype solvated by TIP3P water molecules and counter-ions.